Disturbance Rejection for a Zero-bias Controlled Active Magnetic Bearing Based on Disturbance Observer and Notch Filter

Hai Rong and Kai Zhou

Department of Mechanical Engineering
Tsinghua University, Beijing, 100084, China
rongh14@mails.tsinghua.edu.cn, zhoukai@mail.tsinghua.edu.cn

Abstract **─** This paper introduces a nonlinear disturbance observer plus general notch filter based zero-bias control strategy to handle disturbance and reduce power consumption for the radial magnetic bearing in the magnetically suspended spindle. The zero-bias control is used to decrease the power consumption of magnetic bearings, as large power consumption causes temperature rise of system and temperature drift of sensor. The suspension of the rotor is affected by complicated disturbance including non-periodic and periodic disturbance. In order to reduce the deviation of rotor brought by external disturbance, the nonlinear disturbance observer is used. However, since the response lag to the disturbance, the nonlinear disturbance observer cannot suppress the periodic imbalance force well. Therefore, the general notch filter is introduced to reduce the periodic vibration. The effectiveness on the disturbance suppression and power reduction of the proposed method is verified by experiment results.

Index Terms **─** Active magnetic bearing, disturbance rejection, general notch filter, nonlinear disturbance observer, zero-bias control.

I. INTRODUCTION

As well known, one of the main characteristics of active magnetic bearing (AMB) system is nonlinearity [1–5]. The conventional bias controlled way to handle the high nonlinearity is using the Taylor series expansion to linearize it [1], however, constant bias current is generated. Generally, large bias current is set to improve the stiffness, which causes large copper and eddy current losses, brings the temperature rise of system and temperature drift of sensors [6]. The zero-bias current control algorithm has been proposed to reduce the power consumption of the AMB [7–10]. Sivrioglu adopted the zero-bias control method in the control of a magnetic suspension flywheel [7]. However, the controller is much difficult to design for the zero-bias current control as the system nonlinearity. One linear control structure for a cascaded position-flux controller operating at zero bias is proposed [8], which uses a flux observer to estimate the flux state. A cascaded position-force controller structure is proposed to control the AMB under zero-bias, which means the position controller can use any linear or nonlinear control strategies, and applications adopting the linear algorithms such as H_∞ control [10] can be found in the literature, however, no complicated disturbance is considered.

The suspension of the rotor is affected by kinds of disturbance. For the magnetically suspended spindle, when the cutting tool enters and leaves the work piece, the suspension of the rotor suffers from non-periodic disturbance such as step and impulse forces. However, due to the randomness and uncertainty of disturbance, it is hard to predict and suppress it. $H\infty$ [11] or μ synthesis [12] algorithms have been used in the AMB systems, nevertheless, the high requirement of modeling accuracy and algorithm complexity limit the range of applications. Sliding mode control (SMC) method has been applied in maglev suspension application [13] for the advantages of quick response and insensitivity to parameter uncertainties. Nevertheless, SMC method is short of dealing with disturbance with unknown bound. The adaptive backstepping sliding mode control [14] is therefore proposed to handle the unknown disturbance, whereas, it estimates the disturbance simply via an integral of the state variables, which asymptotically converges slowly, therefore, the disturbance should be slowly varied. Disturbance observer based control (DOBC) approach which combines the disturbance observer with basic control method has been proposed [15–16]. Under this control framework, the normal control part is designed to achieve basic performance for the whole system, while the disturbance observer is developed to eliminate the effects caused by disturbance. With the co-operation of normal control part and disturbance observer, the DOBC approach can handle the non-periodic disturbance well.

Due to the eccentricity from the mass center to the geometric center, the rotation axis of the rotor and the inertial axis cannot coincide, the imbalance force is

Submitted On: December 4, 2018
Accepted On: March 21, 2019

therefore generated. The disturbance observer loses its effectiveness to handle imbalance force as the response lag to the disturbance, especially in high frequencies. There are two main control strategies to handle imbalance force – imbalance compensation and automatic balancing. Automatic balancing is commonly used since it significantly reduces the possibility of saturation of the power amplifier, while imbalance compensation could easily lead to saturation of the power amplifier. Therefore, automatic balancing is the better choice for zero-bias control. Many researches have investigated the active suppression of imbalance vibration, most are based on biased current controlled mode, such as the iterative learning control (ILC) [17]. However, the imbalance suppression methods under zero-bias control are rare in the literature. The generalized notch filters are widely used in the imbalance suppression applications [18], due to the simple structure and easy realization. Therefore, it can be used in the circumstances of zero-bias controlled mode.

In this paper, a new zero-bias control structure of the AMB system based on the nonlinear disturbance observer and generalized notch filter has been proposed and studied, which uses the zero-bias control strategy to reduce power consumption, and achieves suppression of non-periodic disturbance and imbalance vibration force via nonlinear disturbance observer and generalized notch filter respectively. The suspension control law is designed by state feedback control algorithm. Finally, the effectiveness of the proposed method is verified by experiment results.

The paper is organized as follows: Section II focuses on the system model and description; Section III provides the controller design process; Section IV shows the experiment platform and the corresponding experiment results; Conclusions are given in Section V.

II. MODEL OF THE ZERO-BIAS AMB SYSTEM

The radial support system of the magnetically suspended spindle is composed of two radial AMBs. The diagram of the radial AMBs system is shown in Fig. 1. Due to the movement of rotor between the axial and radial degrees can be decoupled, the influence of axial movement to the radial motion can be ignored. Therefore, the dynamic equations of the rotor for the radial four degrees of freedoms (4–DOFs) are:

$$\begin{aligned} \boldsymbol{M\ddot{q}} + \boldsymbol{G\dot{q}} &= \boldsymbol{Bu_f} + \boldsymbol{f_d} \\ \boldsymbol{q_b} &= \boldsymbol{T_s q} \\ \boldsymbol{y} &= \boldsymbol{Cq} \end{aligned} , \quad (1)$$

define the mass matrix $\boldsymbol{M}$, the gyroscopic matrix $\boldsymbol{G}$, the control input matrix $\boldsymbol{B}$, the transform matrix $\boldsymbol{T_s}$, the output matrix $\boldsymbol{C}$, the center of gravity (COG) coordinates $\boldsymbol{q}$, the AMB coordinates $\boldsymbol{q_b}$, the sensor coordinates $\boldsymbol{y}$, the external disturbance $\boldsymbol{f_d}$, the electromagnetic force $\boldsymbol{u_f}$.

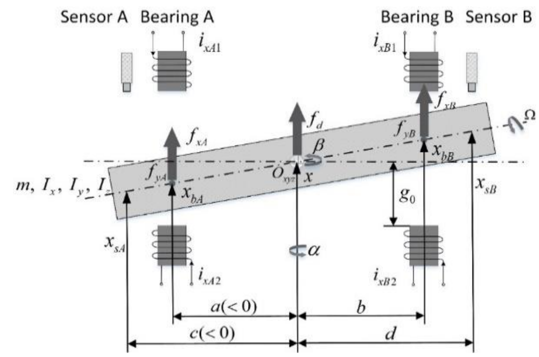

Fig. 1. The diagram of the radial AMBs system.

Since the rotor normally operates within the range of rigid frequencies and the sensor centers are close to the AMB centers, to simplify the modeling process, assume that the output matrix $\boldsymbol{C}$ equals to the transform matrix $\boldsymbol{T_s}$, namely, Equation (1) can be rewritten as:

$$\begin{aligned} \boldsymbol{MT_s}^{-1}\boldsymbol{\ddot{q}_b} + \boldsymbol{GT_s}^{-1}\boldsymbol{\dot{q}_b} &= \boldsymbol{T_s}^{\mathrm{T}}\boldsymbol{u_f} + \boldsymbol{f_d} \\ \boldsymbol{y} &= \boldsymbol{q_b} \end{aligned} . \quad (2)$$

For the slender rotor considered in this research, the transverse mass moments of inertia are significantly larger than the polar mass moment of inertia, the gyroscopic effect and coupling of two AMBs in the same direction can be ignored [18]. Besides, the design parameters for the front and rear AMBs are not the same, the max design force for the front AMB are much larger than the rear AMB, as the front AMB is the main part to bear external load in the radial directions. The suspension accuracy of the front AMB is more important than that of the rear AMB. That means the AMB systems can be modeled separately for each DOF. Since the above reasons, the 4-DOFs AMBs system can be built as the following form:

$$m\ddot{x}_i = b_i f_{ui} + f_{di}, \; i = xA, xB, yA, yB, \quad (3)$$

where, f_{ui} and f_{di} denote the electromagnetic force and the lumped disturbance for each DOF respectively, b_i is the force distribution coefficient. Due to the limits of space, the detail descriptions about the derivation process are not given, more details can be found in Ref. 16. Therefore, decentralized control strategy can be used for two AMBs. Take the front AMB A into consideration, the state space form of the AMB in the AY direction is:

$$\begin{cases} \dot{x}_1 = x_2 \\ \dot{x}_2 = (bf_u + f_d)/m \\ y = x_1 \end{cases}, \quad (4)$$

where, x_1 and x_2 represent the displacement and velocity of the rotor separately, y is system output, f_u denotes the electromagnetic force in AY direction, f_d represents the lumped disturbance (including the equivalent imbalance force, non-periodic external force and the gravity, etc), b is the force distribution coefficient in AY direction, m is the mass of rotor.

Then based on the Maxwell's law, the electromagnetic force can be presented as:

$$f_u = k[\frac{i_1^2}{(g_0 - y)^2} - \frac{i_2^2}{(g_0 + y)^2}],\ k = \frac{\mu_0 A N^2}{4}, \quad (5)$$

where k represents the electromagnetic force coefficient, i_1, i_2 are the coil currents, N is the turn of coil, A is the area of stator pole, g_0 is the normal air gap, μ_0 represents the magnetic field constant in vacuum, which equals to $4\pi\times10^{-7}$ Vs/Am.

From Equations (4) and (5), it can be known that the whole system is a nonlinear one when the coil current is considered as system input. Besides, there are two control outputs whereas only one input, which is not desired. Treat the electromagnetic force as the system input instead of current, then the AMB system becomes a linear one. Therefore, a new equivalent force controlled zero-bias AMB system can be written as:

$$\begin{cases} \dot{x}_1 = x_2 \\ \dot{x}_2 = g(x_1)u + d \\ y = x_1 \end{cases}. \quad (6)$$

Define u as the new system input, $g(x_1) = b/m$ is the input coefficient, and d denotes the lumped disturbance, $d = f_d / m$. Then the excitation current of the coil can be calculated via the following transform relationship:

$$\begin{cases} i_1 = 0, i_2 = (g_0 + y)\sqrt{\frac{u}{k}},\ u \geq 0 \\ i_1 = (g_0 - y)\sqrt{\frac{-u}{k}}, i_2 = 0,\ u < 0 \end{cases}. \quad (7)$$

The zero-bias AMB system in Equation (6) is a linear one, therefore, linear or nonlinear control strategies can be used. To maintain the normal suspension and suppress disturbance well, a DOBC approach is proposed and designed. Before the controller design, define the tracking error and its derivatives as:

$$\begin{aligned} e &= x_1 - x^* \\ \dot{e} &= \dot{x}_1 - \dot{x}^* \\ \ddot{e} &= \ddot{x}_1 - \ddot{x}^* = g(x_1)u + d - \ddot{x}^* \end{aligned}, \quad (8)$$

where x^*, $\dot{x}^*$, $\ddot{x}^*$ are the reference position, velocity and acceleration of the rotor respectively.

Let $\boldsymbol{\lambda} = [\lambda_1 \quad \lambda_2]^T = [e \quad \dot{e}]^T$, then Equation (6) can be written into a state-space form as:

$$\dot{\boldsymbol{\lambda}} = \begin{bmatrix} \lambda_2 \\ g(x_1)u - \ddot{x}^* \end{bmatrix} + \begin{bmatrix} 0 \\ 1 \end{bmatrix} d. \quad (9)$$

Define $\boldsymbol{G_d} = [0 \quad 1]^T$ and,

$$\boldsymbol{\eta} = \begin{bmatrix} \lambda_2 \\ g(x_1)u - \ddot{x}^* \end{bmatrix} = \begin{bmatrix} \eta_1 \\ \eta_2 \end{bmatrix}. \quad (10)$$

Then system Equation (9) changes to:

$$\boldsymbol{\lambda} = \boldsymbol{\eta} + \boldsymbol{G_d} d. \quad (11)$$

III. CONTROLLER DESIGN

A. Nonlinear disturbance observer based state feedback controller design

In order to handle the non-periodic disturbance, a nonlinear disturbance observer (NDO) is proposed [15], which observes the disturbance as well as its derivatives. For the convenience of realization, the first two-order derivatives of disturbance are considered here, and an assumption is made that the feasibility of NDO is existing if only the lumped disturbance meets the following assumption:

Assumption: The lumped disturbance d and its first two-order derivatives are continuous and bounded, namely:

$$|\frac{\partial^j d(t)}{\partial(t)^j}| \leq \mu, \quad for\ j = 0,1,2, \quad (12)$$

where μ is a positive constant, μ can be unknowable.

Based on the definitions and deductions above, the NDO is designed as:

$$\begin{cases} \hat{d} = p_1 + q_1(\lambda_1 + \lambda_2) \\ \dot{p}_1 = -q_1(\eta_1 + \eta_2) - q_1\hat{d} + \hat{\dot{d}} \\ \hat{\dot{d}} = p_2 + q_2(\lambda_1 + \lambda_2) \\ \dot{p}_2 = -q_2(\eta_1 + \eta_2) - q_2\hat{d} \end{cases}, \quad (13)$$

where $\hat{d}$ and $\hat{\dot{d}}$ are estimations of d and its derivative respectively, p_1 and p_2 are auxiliary functions, and q_1, q_2 are positive constants. $\boldsymbol{D}$

Let $\boldsymbol{D} = [d \quad \dot{d}]^T$, then Equation (13) is reformed as:

$$\begin{cases} \hat{\boldsymbol{D}} = \boldsymbol{p} + \boldsymbol{q}(\lambda_1 + \lambda_2) \\ \dot{\boldsymbol{p}} = -\boldsymbol{q}(\eta_1 + \eta_2) + \boldsymbol{Q}\hat{\boldsymbol{D}} \end{cases}, \quad (14)$$

where $\hat{\boldsymbol{D}} = \begin{bmatrix} \hat{d} \\ \hat{\dot{d}} \end{bmatrix}$, $\boldsymbol{p} = \begin{bmatrix} p_1 \\ p_2 \end{bmatrix}$, $\boldsymbol{q} = \begin{bmatrix} q_1 \\ q_2 \end{bmatrix}$, $\boldsymbol{Q} = \begin{bmatrix} -q_1 & 1 \\ -q_2 & 0 \end{bmatrix}$.

According to Equation (14), the derivative of $\hat{\boldsymbol{D}}$ is yielded as:

$$\begin{aligned} \dot{\hat{\boldsymbol{D}}} &= \dot{\boldsymbol{p}} + \boldsymbol{q}(\dot{\lambda}_1 + \dot{\lambda}_2) \\ &= -\boldsymbol{q}(\eta_1 + \eta_2) + \boldsymbol{Q}\hat{\boldsymbol{D}} + \boldsymbol{q}(\eta_1 + \eta_2 + d) \\ &= \boldsymbol{Q}\hat{\boldsymbol{D}} + \boldsymbol{q}d \end{aligned}. \quad (15)$$

Then the estimation error can be defined as follows:

$$\tilde{\boldsymbol{D}} = [\tilde{d} \quad \tilde{\dot{d}}]^T = \boldsymbol{D} - \hat{\boldsymbol{D}}. \quad (16)$$

The observer error dynamics can be written as

$$\begin{aligned}\dot{\tilde{\boldsymbol{D}}} &= \dot{\boldsymbol{D}} - \dot{\hat{\boldsymbol{D}}} \\ &= \begin{bmatrix}\dot{d} & \ddot{d}\end{bmatrix}^{\mathrm{T}} - (\boldsymbol{Q}\hat{\boldsymbol{D}} + \boldsymbol{q}d), \\ &= \boldsymbol{Q}\tilde{\boldsymbol{D}} + \boldsymbol{E}\ddot{d}\end{aligned} \quad (17)$$

where $\boldsymbol{E} = [0 \quad 1]^T$.

Suppose that q_1 and q_2 are chosen to guarantee that the eigenvalues of $\boldsymbol{Q}$ are in the left hand plane (LHP), then for any given positive definite matrix $\boldsymbol{R}$, a positive definite symmetric matrix $\boldsymbol{P}$ can be found to satisfy the following relationship:

$$\boldsymbol{Q}^T\boldsymbol{P} + \boldsymbol{P}\boldsymbol{Q} = -\boldsymbol{R}, \quad (18)$$

then the observer is asymptotically stable. The details of stability analysis can be seen in Ref. 15. Therefore, the norm of the extended disturbance estimation error $\tilde{\boldsymbol{D}}$ is ultimately bounded and the bounds can be lowered by choosing q_1, q_2, $\boldsymbol{P}$ and $\boldsymbol{R}$ appropriately.

Remark: The NDO has strong ability to handle disturbance since the derivative of the disturbance is also estimated. Meanwhile, it should be mentioned that the bound of disturbance is unnecessary to know. Since that, stronger ability to handle non-periodic disturbance can be expected. Though the bound value can be unknown, in fact, it affects the suspension accuracy of the rotor a lot. Therefore, strategies to lower the bound value such as removing the gravity from the unknown disturbance are meaningful.

With the disturbance observer, the equivalent disturbance for the system becomes $\tilde{d}$, which is much smaller than d, then the system can be presented as the following state space form:

$$\begin{aligned}\dot{\boldsymbol{x}} &= \boldsymbol{A}\boldsymbol{x} + \boldsymbol{B}u + \boldsymbol{G_d}\tilde{d} \\ y &= \boldsymbol{C}\boldsymbol{x}\end{aligned}, \quad (19)$$

where $\boldsymbol{x} = \begin{bmatrix} x_1 \\ x_2 \end{bmatrix}, \boldsymbol{A} = \begin{bmatrix} 0 & 1 \\ 0 & 0 \end{bmatrix}, \boldsymbol{B} = \begin{bmatrix} 0 \\ g(x_1) \end{bmatrix}, \boldsymbol{C} = \begin{bmatrix} 0 \\ 1 \end{bmatrix}^T$.

Also system (11) changes to:

$$\dot{\boldsymbol{\lambda}} = \boldsymbol{\eta} + \boldsymbol{G_d}\tilde{d}. \quad (20)$$

According to the DOBC design framework [15], the structure of the controller for the zero-bias AMB system can be divided into two parts – the disturbance compensation part and the normal suspension part. As the effect caused by the unknown disturbance is eliminated via disturbance observer, then a suspension controller needs to be designed.

Based on the state feedback control law [19], it can be deduced that the whole system is controllable. Then a state feedback controller is deigned to realize the normal suspension of rotor.

$$u_f = -\boldsymbol{K}\boldsymbol{\lambda}, \quad (21)$$

where, $\boldsymbol{K} = \begin{bmatrix} k_1 & k_2 \end{bmatrix}$ is the feedback coefficient matrix.

Then the whole control output can be presented as:

$$\begin{aligned}u &= u_f + u_b \\ &= -\boldsymbol{K}\boldsymbol{\lambda} - \hat{d} / g(x_1)\end{aligned}, \quad (22)$$

where u and u_b are the whole control output and the output of the disturbance observer. The DOBC method combining nonlinear disturbance observer with state feedback control can be abbreviated as SF+NDO.

B. The general notch filter based imbalance force rejection controller design

Although the disturbance observer can well restrain disturbance, the state feedback controller based on disturbance observer itself is still feedback closed-loop control, that means there remains response lag to the disturbance, and with the increase of disturbance frequency, the response lag is more obvious. Therefore, the disturbance observer functions as a low-pass filter, it is only effective on the low frequency range, and it cannot handle the imbalance force well under high spinning speed. Besides, the value of the unknown upper bound of disturbance μ affects the accuracy of suspension a lot. With the limits of response frequency of the power amplifier, the generalized notch filter (GNF) based minimum current compensation control strategy is therefore proposed to deal with the periodic imbalance force. The principle of the GNF N is shown in Fig. 2. The core of the notch filter is the notch feedback item N_f, its central frequency can vary with the change of rotating speed, the convergence factor ε determines the convergence rate and bandwidth of the notch filter.

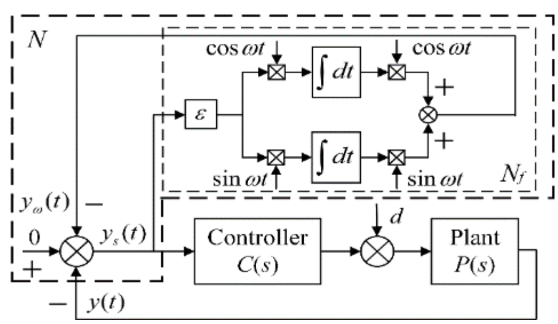

Fig. 2. The principle of the generalized notch filter N.

Assume $y_s(t)$ and $y_\omega(t)$ to be the input and output of the notch feedback item respectively, then $y_\omega(t)$ equals to:

$$y_\omega(t) = \varepsilon\left[\sin\omega t \quad \cos\omega t\right]\begin{bmatrix}\int y_s(t)\sin\omega t dt \\ \int y_s(t)\cos\omega t dt\end{bmatrix}. \quad (23)$$

The transfer function of the notch feedback item can be written as

$$N_f(s) = \frac{Y_\omega(s)}{Y_s(s)} = \frac{\varepsilon s}{s^2 + \omega^2}. \quad (24)$$

Then transfer function from system output $Y(s)$ to the notch filter output $Y(s)$ is:

$$N(s) = \frac{Y_s(s)}{Y(s)} = \frac{s^2 + \omega^2}{s^2 + \varepsilon s + \omega^2}. \quad (25)$$

When $\varepsilon \neq 0$, let $s = j\omega_r$, the following equation can be established:

$$\begin{cases} N(j\omega_r) \approx 1, & \left[\omega_r \in (0,\ \omega - \Delta\omega) \cup (\omega + \Delta\omega,\ \infty)\right] \\ N(j\omega_r) = 0, & \left[\omega_r \in (\omega - \Delta\omega,\ \omega + \Delta\omega)\right] \end{cases}. \quad (26)$$

Therefore, as long as $\varepsilon \neq 0$, the output of the notch feedback item tends to the component with the frequency of ω in the system output $y(t)$. By subtracting the original displacement signal to the signal estimated by the notch filter, the same frequency component caused by the imbalance force in the original signal $y(t)$ is filtered out, in other words, the same frequency current generated by the controller is eliminated, and thus the imbalance force is suppressed.

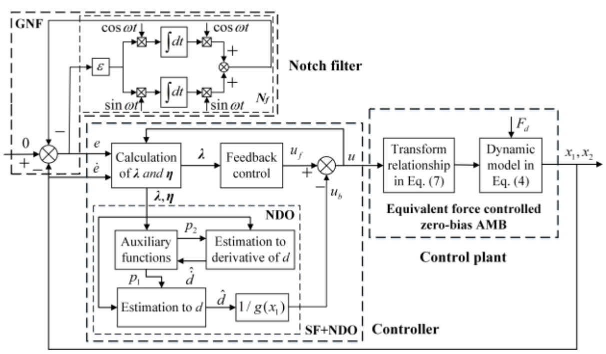

Fig. 3. The whole control system based on SF+NDO+GNF.

Since that, with the co-function of the disturbance observer and the notch filter, the imbalance force and non-periodic disturbance can be well restrained. The whole control system for nonlinear disturbance observer based state feedback control plus general notch filter (SF+NDO+GNF) is described as Fig. 3.

IV. EXPERIMENTS

A. Experimental platform construction

As shown in Fig. 4, a 5 degree of freedoms (5–DOFs) magnetically suspended spindle system is built, which consists of two radial AMBs, one axial AMB and the drive motor mainly. Figure 5 shows the structure of the front radial AMB. In this paper, the main attention is paid on the front AMB, for which is the main part to bear external load in the radial directions. The whole control system for the magnetic bearing is based on a FPGA chip – the EP4CE15F17C8 manufactured by ALTERA. The proposed control methods employ the cascaded structure with position and current feedback. As well known, for the zero-bias control, the magnetic force slue rate near the origin is zero. In order to produce a small force, a large change is needed in control current. To overcome this problem, firstly, large current (equals to 20 A) and small turns of coil (equals to 40) for AMB are designed to improve the force bandwidth of actuators, then hysteretic current control is adopted to realize the fast response of current, therefore the largest force bandwidth can be held. Parameters of the front radial AMB system are shown in Table 1.

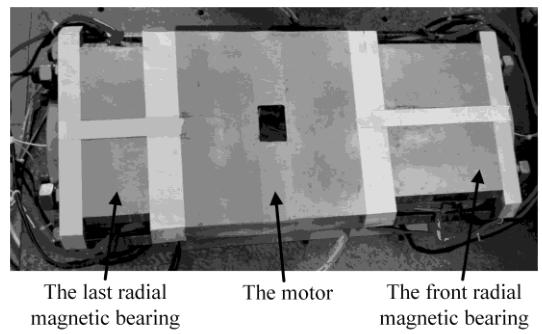

Fig. 4. 5–DOFs magnetically suspended spindle system.

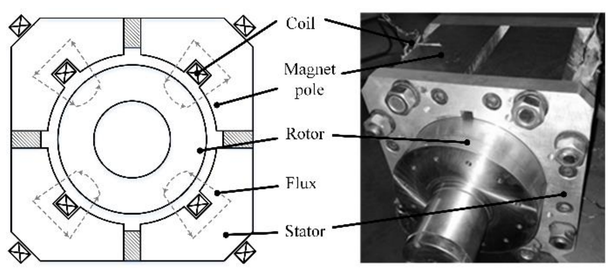

Fig. 5. The structure of the front radial AMB.

Table 1: Parameters of the front radial AMB system

Parameter (Symbol)	Value
Mass of the rotor (m)	55 kg
Transverse mass moments of inertia (I_x, I_y)	0.817 kg×m^2
Polar mass moment of inertia (I_z)	0.139 kg×m^2
Magnetic pole area (A)	5.04×10^{-3} m^2
Electromagnetic force coefficient (k)	2.53×10^{-6} N×m^2/A^2
Nominal air gap (g_0)	0.3 mm
Auxiliary gap (g_a)	0.1 mm
Turns of coil (N)	40
Max current (i_{max})	20 A

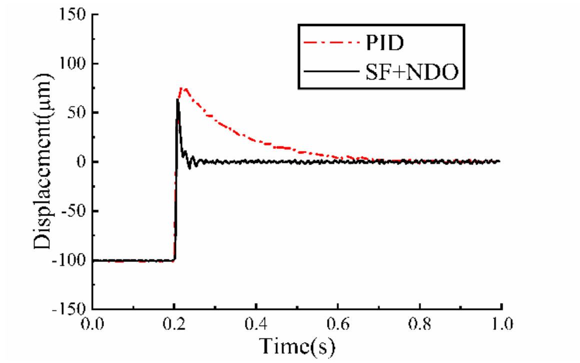

Fig. 6. Displacement curves during initial lift up.

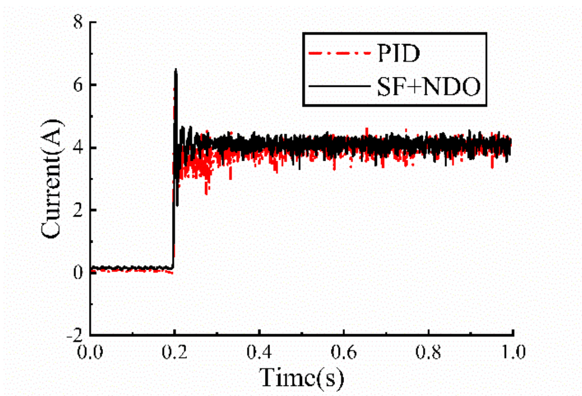

Fig. 7. Current curves during initial lift up.

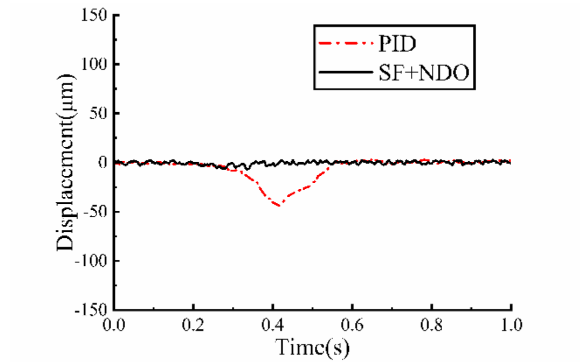

Fig. 8. Displacement curves under the constant load.

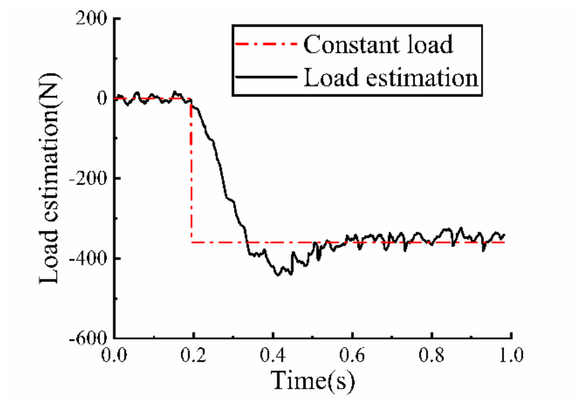

Fig. 9. Load estimation curve under the constant load.

B. Experimental tests for SF+NDO based control

Firstly, researches on the non-periodic disturbance rejection are carried out under static condition. The effectiveness of the SF+NDO control is verified under two kinds of circumstances, namely the initial lift up process and adding a constant load. In order to verify the effectiveness of the proposed algorithm, the commonly used proportional-integral-derivative (PID) strategy is compared. Figures 6–8 show the displacement and current curves under two kinds of disturbance in Y direction respectively. Firstly, Fig. 6 shows the displacement curves during initial lift up process, the maximum overshoots and adjusting time of the rotor for the SF+NDO method and PID are 63 μm / 0.06 s and 75 μm / 0.52 s respectively. It is demonstrated in Fig. 8 that when a 360 N constant load is applied to the rotor, the maximum deviations and recovery time of the rotor for SF+NDO and PID are 7 μm / 0.25 s and 44 μm / 0.4 s respectively. Therefore, compared with PID control strategy, the SF+NDO control strategy has stronger ability to restrain the non-periodic disturbance. In addition, the load estimation curve for the disturbance observer can be obtained as shown in Fig. 9.

Then, at 2400 rpm, the dynamic performances for the SF+NDO method and PID control are compared. Figure 10 describes the displacement curves in Y direction. It is demonstrated that the maximum deviations of the rotor for SF+NDO and PID are 9 μm and 17 μm respectively. Therefore, it can be seen that the SF+NDO control strategy can suppress the harmonic vibrations well. Though the proposed SF+NDO method can suppress disturbance, there are still residual vibrations caused by the imbalance force, as described in Fig. 11. Therefore, a new strategy is needed to suppress the imbalance force.

C. Experimental tests for SF+NDO+GNF based control

On the basis of the SF+NDO method, the imbalance force is further suppressed by introducing the GNF. At 2400 rpm, the performances of suspension under the three kinds of methods are obtained, as shown in the Fig. 12. The results demonstrate that the basic values of displacement are about 2.4 μm, 2.0 μm and 0.85 μm for PID, SF+NDO and SF+NDO+GNF respectively. Finally, the proposed SF+NDO+GNF method is compared with biased control (the biased current is 4A) using PID method at the same speed, and it shows in Fig. 13 that the vibrations also decreased with the proposed method.

Besides, the copper losses for the front radial magnetic bearing are calculated for the proposed control method and biased control method (the biased current is 4A) respectively, Fig. 14 shows the relationship between copper losses and the rotating speed. It demonstrates that zero bias control reduces the power consumption by at least 40% compared with the biased control. Therefore, zero bias control is helpful to increase the running time of AMB system.

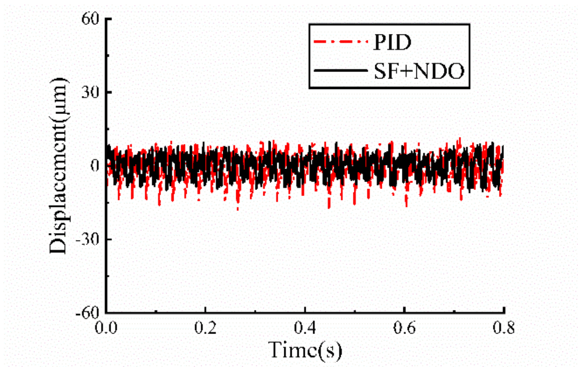

Fig. 10. Displacement curves at 2400 rpm.

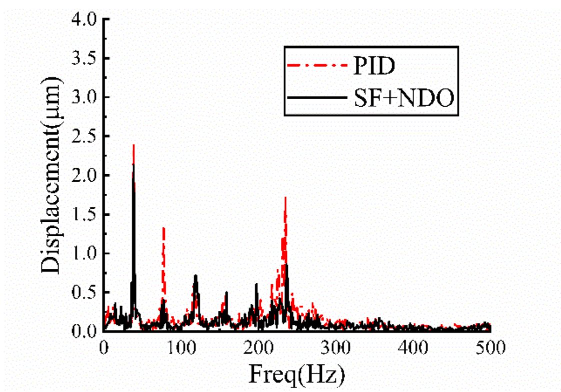

Fig. 11. The spectrum curves of displacement at 2400 rpm.

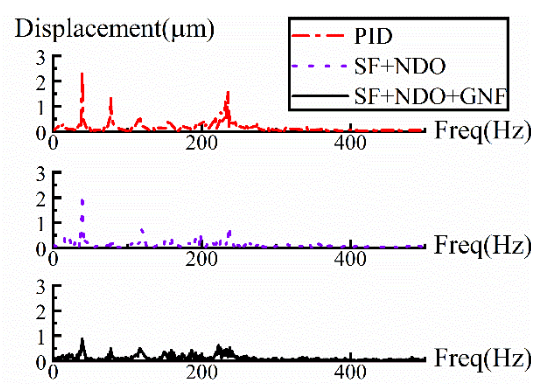

Fig. 12. The spectrum curves of displacement for the three methods at 2400 rpm.

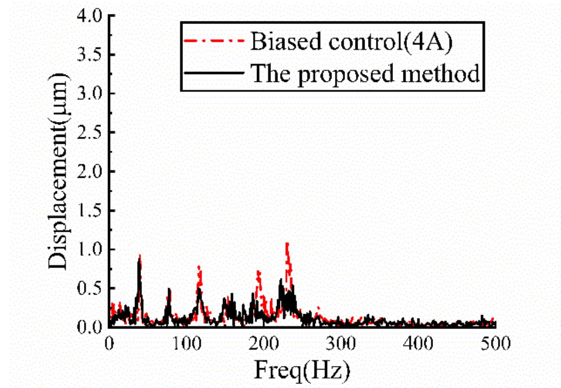

Fig. 13. The spectrum curves of displacement for biased control and the proposed method at 2400 rpm.

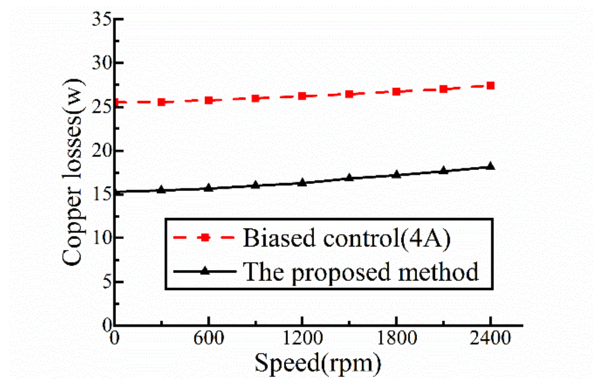

Fig. 14. Copper losses for biased control and the proposed method.

From above, it can be seen that the proposed SF+NDO+GNF method for zero bias controlled AMB system shows excellent performance on comprehensive disturbance suppression and power reduction. Therefore, the effectiveness of the proposed method is verified.

V. CONCLUSIONS

In this paper, a nonlinear disturbance observer plus notch filter based zero-bias control strategy is proposed for the radial AMBs in a magnetically suspended spindle. An equivalent electromagnet force controlled model is introduced to handle the nonlinearity brought by zero-bias current strategy. The nonlinear disturbance observer is adopted to restrain the non-periodic disturbance such as step forces. The periodic imbalance force is suppressed by introducing the general notch filter. Various experiments have been performed to verify the effectiveness of the approach. Besides, the proposed SF+NDO+GNF method is compared with biased control using PID method, it also show excellent performance in vibrations suppression and power reduction. Since the strong ability both in power reduction and disturbance restraint for the proposed method, it can also be adopted to other AMB applications where low power consumption and suppression of disturbance are needed.

ACKNOWLEDGMENT

This work was supported in part by the National Natural Science Foundation of China (Grant No. 51275257).

REFERENCES

[1] G. Schweitzer and E. H. Maslen, *Magnetic Bearings: Theory, Design, and Application to Rotating Machinery*. Berlin Heidelberg: Springer–Verlag, 2009.

[2] S. L. Chen and K. Y. Liu, "Sensorless control for a three-pole active magnetic bearing system," *ACES Journal*, vol. 32, no. 8, pp. 720-725, Aug. 2017.

[3] L. L. Zhang and J. H. Huang, "Stability analysis for a flywheel supported on magnetic bearings with delayed feedback control," *ACES Journal*, vol. 32, no. 8, pp. 642-649, Aug. 2017.

[4] C. Dumont, V. Kluyskens, and B. Dehez, "Performance of yokeless heteropolar electrodynamic bearings," *ACES Journal*, vol. 32, no. 8, pp. 685-690, Aug. 2017.

[5] Z. Jun, D. D. Song, Q. L. Han, J. M. Wang, G. H. Li, and S. L. Li, "Optimization of T-shaped suspension magnetic ring for vertical axis wind turbine," *ACES Journal*, vol. 33, no. 7, pp. 781-789, July 2018.

[6] D. G. Li, S. Q. Liu, and B. Bian, "Automatic thermal expansion compensation of the precise grinding machine AMB spindle," *Applied Mechanics and Materials*, vol. 130-134, no. 2, pp. 3221-3224, 2011.

[7] S. Sivrioglu, "Adaptive backstepping for switching control active magnetic bearing system with vibrating base," *IET Control Theory and Applications*, vol. 1, no. 4, pp. 1054-1059, 2007.

[8] R. P. Jastrzebski, A. Smirnov, A. Mystkowski, and O. Pyrhönen, "Cascaded position-flux controller for an AMB system operating at zero bias," *Energies*, vol. 7, no. 6, pp. 3561-3575, 2014.

[9] A. Mystkowski and E. Pawluszewicz, "Nonlinear position-flux zero-bias control for AMB system with disturbance," *ACES Journal*, vol. 32, no. 8, pp. 650-656, Aug. 2017.

[10] S. Sivrioglu, K. Nonami, and M. Saigo, "Low power consumption nonlinear control with H∞ compensator for a zero-bias flywheel AMB system," *Journal of Vibration and Control*, vol. 10, no. 8, pp. 1151-1166, 2004.

[11] F. Matsumura, T. Namerikawa, K. Hagiwara, and M. Fujita, "Application of gain scheduled H ∞ robust controllers to a magnetic bearing," *IEEE Transactions on Control System Technology*, vol. 4, no. 5, pp. 484-493, 1996.

[12] M. Chen and C. R. Knospe, "Control approaches to the suppression of machining chatter using active magnetic bearings," *IEEE Transactions on Control Systems Technology*, vol. 15, no. 2, pp. 220-232, 2007.

[13] M. S. Kang, J. Lyou, and J. K. Lee, "Sliding mode control for an active magnetic bearing system subject to base motion," *Mechatronics*, vol. 20, no. 1, pp. 171-178, 2010.

[14] H. Rong and K. Zhou, "Nonlinear zero-bias current control for active magnetic bearing in power magnetically levitated spindle based on adaptive backstepping sliding mode approach," *Proceedings of the Institution of Mechanical Engineers Part C Journal of Mechanical Engineering Science*, vol. 231, no. 20, pp. 3753-3765, 2017.

[15] D. Ginoya, P. D. Shendge, and S. B. Phadke, "Sliding mode control for mismatched uncertain systems using an extended disturbance observer," *IEEE Transactions on Industrial Electronics*, vol. 61, no. 4, pp. 1983-1992, 2014.

[16] L. F. Xiao and Y. Zhu, "Sliding mode output feedback control based on tracking error observer with disturbance estimator," *ISA Transactions*, vol. 53, no. 4, pp. 1061-1072, 2014.

[17] B. Shafai, S. Beale, P. Larocca, and E. Cusson, "Magnetic bearing control systems and adaptive forced balancing," *IEEE Transactions on Control Systems Technology*, vol. 14, no. 2, pp. 4-13, 1994.

[18] Q. Chen, G. Liu, and S. Q. Zheng, "Suppression of imbalance vibration for AMBs controlled driveline system using double-loop structure," *Journal of Sound and Vibration*, vol. 337, pp. 1-13, 2015.

[19] H. Wei, Y. C. Ouyang, and J. Hong, "Vibration control of a flexible robotic manipulator in the presence of input deadzone," *IEEE Transactions on Industrial Informatics*, vol. 13, no. 1, pp. 48-59, 2017.

Hai Rong was born in 1993. He received B.S. degree in Mechanical Engineering and Automation from Huazhong University of Science and Technology (HUST) in 2014. He is currently pursuing a Ph.D. degree in Tsinghua University. His research focuses on magnetic bearing control and magnetic bearing systems design.

Kai Zhou was born in 1954. He received Ph.D. degree in Mechanical Engineering from Tsinghua University. He is currently a Full Professor in the Department of Mechanical Engineering, Tsinghua University. His research focuses on magnetically suspended systems, CNC systems, high speed motors and servo control.